Bevacizumab Radioimmunotherapy (RIT) with Accelerated Blood Clearance Using the Avidin Chase

Ryan Yudistiro,[†] Hirofumi Hanaoka,*,[‡] Natsumi Katsumata,[†] Aiko Yamaguchi,[‡] and Yoshito Tsushima[†,§]
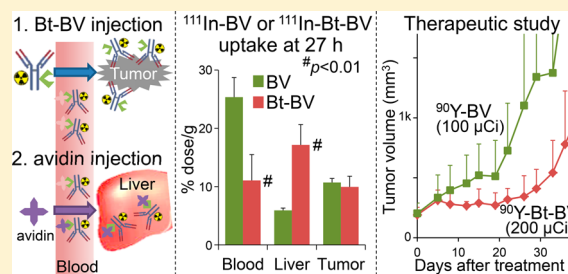
[†]Department of Diagnostic Radiology and Nuclear Medicine and [‡]Department of Bioimaging Information Analysis, Gunma University Graduate School of Medicine, 3-39-22 Showa, Maebashi 371-8511, Japan

[§]Research Program for Diagnostic and Molecular Imaging, Division of Integrated Oncology Research, Gunma University Initiative for Advanced Research (GIAR), 3-39-22 Showa, Maebashi 371-8511, Japan

S Supporting Information

ABSTRACT: The overexpression of vascular endothelial growth factor (VEGF) in varying types of solid tumor renders radioimmunotherapy (RIT) with the anti-VEGF antibody bevacizumab (BV) a promising treatment. However, the slow blood clearance of BV, which may increase the occurrence risk of hematotoxicity, hinders the application of BV-RIT. Using the avidin chase is a long-known blood clearance enhancement strategy for biotinylated-mAb. To enhance RIT efficacy by increasing the radioactivity dose, we evaluated the ability of avidin to accelerate the blood clearance of yttrium-90 (^{90}Y)-labeled biotinylated BV (^{90}Y-Bt-BV) in a xenograft

mouse model of triple-negative breast cancer (TNBC). The biodistribution study in the TNBC xenograft mice confirmed the high and specific tumor accumulation of the indium-111 (^{111}In)-BV. The blood clearance enhancement effect of the avidin chase was demonstrated in the normal mouse studies with ^{111}In-Bt-BV. In the subsequent biodistribution studies with the tumor-bearing mice, an optimized dose of avidin injection subsequent to ^{111}In-Bt-BV with an appropriate biotin valency successfully accelerated the blood clearance of ^{111}In-Bt-BV without impairing its tumor accumulation level. The avidin chase enabled an increase in the maximum tolerated dose of ^{90}Y-Bt-BV to twice as much as that of ^{90}Y−BV in tumor-bearing mice and thereby significantly improved the therapeutic effect of ^{90}Y-Bt-BV compared to ^{90}Y−BV ($p < 0.05$). These results underscored the potential usefulness of ^{90}Y-bevacizumab-RIT with the avidin chase for the treatment of VEGF-positive tumors.

KEYWORDS: bevacizumab, radioimmunotherapy, avidin chase, blood clearance, triple-negative breast cancer

INTRODUCTION

With the outstanding achievements of radiolabeled monoclonal antibodies (mAbs) in treating hematological malignancies, interest in radioimmunotherapy (RIT) has grown as an attractive approach for solid tumors.[1,2] As the carrier of radionuclides in RIT, the prerequisite for mAbs is high tumor-targeting specificity and affinity rather than the antitumor effect itself. This means that mAbs against many types of tumor-associated antigens can be potential candidates for RIT. A promising target is vascular endothelial growth factor (VEGF), one of the hallmarks of cancer.[3,4] Although VEGF is a secreted protein, it is retained in the tumor tissue, and thus the preclinical as well as clinical success of radiolabeled bevacizumab (a clinically used anti-VEGF antibody) in radioimmunoimaging and RIT has been reported.[5−9] Considering wide application of bevacizumab for substantial kinds of cancer,[10,11] clinical use of bevacizumab-RIT is awaited.

However, in contrast to the high effectiveness of RIT in hematological malignancies, the clinical success of RIT for solid tumors is modest. This is due mainly to the relationship between the therapeutic effect and hematotoxicity.[2] The large

molecular size of the IgGs, that is, 150 kDa, prolongs their circulation time and thus increase the risk of hematopoietic and other normal organ toxicity.[12] Because bevacizumab has an even longer terminal biological half-life compared to other mAbs (approximately 20 days, range 11−50 days in patients),[13,14] a blood clearance enhancement strategy is necessary for the application of bevacizumab RIT in clinical settings.

Currently, blood clearance enhancement approaches rely on the smaller molecular sizes of radiolabeled compounds.[12,15,16] While the use of fragmented antibodies effectively enhances blood clearance compared to IgG, the advantage of these antibodies is limited because their simultaneously decreased tumor accumulation level compromises the therapeutic effect. In a pretargeting strategy, by contrast, the high radioactivity level in the tumor is maintained because the tumor is preloaded

with nonradiolabeled antibodies, and subsequently, antibody-reactive radiolabeled small molecules are delivered.[17,18] The radioactivity level in the tumor relies on the uptake level of nonradiolabeled mAbs, whereas the blood clearance rate depends on the rapid elimination pattern of the radiolabeled small molecule. However, if an antibody has an extremely slow blood clearance rate, an additional step, the injection of a 'clearing agent', is necessary.[17,19] If antibodies remain in the circulation, they prevent radiolabeled small molecules from binding to the antibodies located in the tumor by trapping the radiolabeled small molecules in the circulation. Therefore, it is desirable to develop a more simple and effective strategy as an alternative to this complex and troublesome three-step pretargeting RIT.

Another effective strategy for increasing therapeutic index by reducing hematopoietic toxicity is the removal of radiolabeled antibody from circulation such as "chase" and extracorporeal depletion.[20,21] In the chase strategy, molecules directly recognize radiolabeled antibody such as secondary antibody or avidin for biotinylated antibody are injected.[20,22] Studies in tumor bearing mice reported the dramatic decrease in the blood radioactivity following avidin chase.[20,23−25] However, while a number of pretargeting RIT studies harnessing avidin−biotin system, avidin chase strategy for RIT has rarely been performed. No study applied the avidin chase strategy for RIT with yttrium-90 (^{90}Y)-labeled antibody. Nevertheless, avidin chase would exert powerful effect for antibodies with slow clearance rate like bevacizumab. In this study, we performed therapeutic studies of ^{90}Y-labeled biotinylated bevacizumab (^{90}Y-Bt-BV), followed by avidin chase in a xenograft model of triple-negative breast cancer (TNBC), which is a bevacizumab-avid and notoriously refractory type of tumor.[26,27] We evaluated the utility of avidin chase for accelerating the blood clearance of ^{90}Y-Bt-BV, and we assessed the potential of the strategy to enhance the efficacy of RIT by increasing the radioactivity dose.

MATERIALS AND METHODS

Conjugation and Radiolabeling of Monoclonal Antibodies. Bevacizumab (BV) was purchased from Chugai Pharmaceutical (Tokyo), and a murine anti-CD20 mAb, NuB2, was purchased from Immuno-Biological Laboratories (Fujioka, Japan). We used 2-(4-isothiocyanatobenzyl)-diethylenetriaminepentaacetic acid (SCN-Bn-DTPA; Macrocyclics, Dallas, TX) for the indium-111 (^{111}In) or ^{90}Y labeling of the mAbs. Typically, SCN-Bn-DTPA in dimethylformamide was added to mAb (5 mg/mL in 50 mM borate-buffered saline, pH 8.5) at the molar ratio of 5:1 and incubated for 24 h at 37 °C. The DTPA-mAbs were purified using a Bio-Spin column (Bio-Rad Laboratories, Hercules, CA) eluted with phosphate-buffered saline (PBS). The number of DTPA attached per molecule of mAb was determined as 1.1, according to the procedure described previously.[28]

The biotinylated-DTPA-BV (DTPA-Bt-BV) was prepared by conjugation of 6-[6-(biotinylamino)hexanoylamino]hexanoic acid N-hydroxysuccinimide ester (Dojindo, Kumamoto, Japan) with amine group of antibody in 0.1 M borate buffer (pH 8.5) at the molar ratio of 3:1, 6:1, or 10:1 overnight at 37 °C. The DTPA-Bt-BV was purified as described above.

The average number of biotin molecules per mAb was determined by performing a 4′-hydroxyazobenzene-2-carboxylic acid (HABA) assay.[29] The mixture of HABA (1.4 mg/mL)/avidin (2.5 mg/mL) in 10 μL of phosphate buffer was added with 5 μL of phosphate buffer solution of DTPA-Bt-BVs. After a 5 min incubation, the absorbance at 500 nm was measured with a spectrophotometer (NanoDrop ND-1000, ThermoFisher Scientific, Waltham, MA). The biotin concentration of each DTPA-Bt-BV was calculated in a comparison with a standard curve using the absorbance of the mixtures with a known concentration of biotin. The protein concentration was also determined based on the absorbance at 280 nm, and then the biotin valencies (biotin number per mAb) were calculated based on the ratio of molar concentrations. The reaction of biotin and DTPA-BV at the molar ratio of 3:1, 6:1, and 10:1 resulted in the biotin valencies of 2.0, 3.5 ± 0.5 (n = 3), and 7.1, respectively (hereinafter referred to as DTPA-Bt$_{2.0}$-BV, DTPA-Bt$_{3.5}$-BV, and DTPA-Bt$_{7.1}$-BV, respectively).

Radiolabeling of Monoclonal Antibodies. For the preparation of the ^{111}In- or ^{90}Y-labeled mAbs, 40 μL (0.37−1.85 MBq) of ^{111}InCl$_3$ solution (Nihon Medi-Physics, Tokyo) or 20−60 μL (74−296 MBq) of ^{90}YCl$_3$ solution (Nucleic, Braunschweig, Germany) was incubated in 0.25 M acetate buffer (pH 5.5, 60, or 200 μL, respectively) for 5 min at room temperature, followed by incubation with DTPA-mAbs (10 μg or 200−800 μg in 0.1 M phosphate buffer, respectively) for 1 h at 37 °C. To trap unconjugated radiometals, 3−5 μL of 100 mM EDTA was added to the reaction mixture.

Iodine-125-labeled BV was prepared according to the standard protocols for the chloramine-T method[30] with slight modification. Briefly, 3.7 MBq/2 μL of Na^{125}I (PerkinElmer, Waltham, MA) and 1 μg of chloramine-T in 1 μL of 0.3 M phosphate buffer (pH 7.4) were added to 40 μg of antibody in 100 μL of 0.3 M phosphate buffer and incubated for 10 min at room temperature. The radiolabeled mAbs were purified as described above. For the purification of ^{90}Y-labeled mAbs, a PD-10 column (GE Healthcare Biosciences AB, Piscataway, NJ) was used instead of the Biospin column. The radiochemical purity of all radiolabeled mAbs after purification was >95%, determined based on the results of Tec-Control Chromatography Strips (Biodex Medical Systems, Shirley, NY). In case of ^{111}In- or ^{90}Y-labeled mAbs, 3 μL of 100 mM EDTA was added to the reaction mixture to trap unconjugated radiometals. One drop of the reaction mixture was spotted on the strip, then the strip was developed with saline. R_f values of radiolabeled antibody and free ^{125}I, ^{111}In-EDTA, or ^{90}Y-EDTA were 0 and 1, respectively. The radiochemical yield of ^{111}In-labeled BV, ^{90}Y-labeled BV, and ^{125}I-labeled BV were >90% (n > 10), 88.8 ± 9.1% (n = 5, mean ± SD), and 87.0%, respectively. The specific radioactivity of the purified ^{111}In-labeled BV, ^{90}Y-labeled BV, and ^{125}I-labeled BV were 37−185 MBq/mg mAb, 290−520 MBq/mg mAb, and 64.4 MBq/mg mAb, respectively.

Immunoreactivity Evaluation. Recombinant human VEGF$_{165}$ was purchased from HumanZyme (Chicago, IL). The VEGF$_{165}$-coated 96-well plate was prepared as described by Chang et al.[31] with slight modification (VEGF$_{165}$ concentration of 3 μg/μL). A mixture of ^{125}I−BV (0.5 kBq/0.001 μg) and serial amounts of unlabeled DTPA-BV, DTPA-Bt$_{2.0}$-BV, DTPA-Bt$_{3.5}$-BV, or DTPA-Bt$_{7.1}$-BV (0.01−100 μg) were added to each well and incubated for 2 h at room temperature. The wells were then washed with 200 μL of PBS three times, and the radioactivity of each well was counted using a well-type gamma counter (ARC7001; Hitachi Aloka Medical, Tokyo).

Tumor Xenograft Mouse Model Preparation. All animal experiments were approved by the animal experiments committee of Gunma University. The TNBC cell line with high

VEGF expression level, MDA-MB-231,[32] was purchased from American Type Culture Collection (Manassas, VA). The cultured cell was harvested and suspended in a mixture of PBS and Matrigel (Corning Life Sciences, Corning, NY) at a 1:1 (v/v) ratio. The cell suspension (5×10^6 cells/100 μL/ mice) was injected into the right dorsal flank of 6-week-old female BALB/c nude mice (Japan SLC, Shizuoka, Japan). The tumor volume was measured twice a week with a caliper, and the tumor volume was calculated as tumor volume = 1/2 (length $\times$ width^2). The mice were used for the biodistribution studies or therapeutic studies when the tumor volume reached 150–250 mm^3.

Immunohistochemistry. The expression levels of VEGF in the MDA-MB-231 xenograft tumor was analyzed by immunohistochemical staining. Tumor xenografts excised from nude mice were embedded in O.C.T. compound (Sakura Finetek Japan, Tokyo) and frozen at −80 °C. Cryosections (6-μm) were immunostained with a rabbit anti-VEGF-A primary antibody (ab46154, Abcam, Cambridge, UK). Immunostaining was detected with a mouse antirabbit secondary antibody (IgG-PerCP: sc-45098, Santa Cruz Biotechnology, Dallas, TX). The sections were counterstained with hematoxylin solution. Negative controls were obtained by omitting the primary antibody.

Biodistribution Studies. We performed four types of biodistribution studies in either tumor xenograft mice or normal ddY mice (Japan SLC) with ^{111}In-labeled mAbs as a surrogate for ^{90}Y-labeled mAbs.[33,34] All mice were fed with normal diet (contains 27 μg of biotin/100 g of pellet). A summary of biodistribution studies is provided as Figure 1. In all studies, radiolabeled antibody and avidin were injected intravenously via tail vein. The tissues of interest were dissected out and weighed at the indicated time after tracer injection, and then the radioactivity was measured by a well-type gamma counter. The accumulation of the tracers is expressed as a percentage of the injected dose per gram of tissue. Radiation-

effective doses for humans were calculated from the biodistribution data of tumor-bearing mice using the software program OLINDA/EXM (version 1.1; Vanderbilt University, Nashville, TN).[35]

Study 1: Evaluation of Biodistribution Profiles and Tumor Specificity of ^{111}In−BV in MDA-MB-231 Tumor Xenograft Mice. One-hundred microliters of ^{111}In-labeled DTPA-BV (^{111}In−BV, 20 kBq/20 μg of mAb) was injected into the tumor-bearing mice. Radioactivity uptakes were determined at 1, 24, 72, and 168 h after injection. To evaluate the specificity of ^{111}In−BV to the xenograft tumor, we injected the mice with ^{111}In-DTPA-BV in the presence of unlabeled antibody (20, 100, or 500 μg/mouse) and sacrificed at 72 h after injection. The radioactivity uptake of ^{111}In-DTPA-NuB2 was also evaluated at 1, 24, and 72 h after injection of 100 μL aliquot of ^{111}In-DTPA-NuB2 (20 kBq/20 μg of mAb).

Study 2: Effect of Biotin Valency and Clearing Agent Injection on Biodistribution Profiles of ^{111}In-Bt(n)-BV. We evaluated the biodistribution profiles of ^{111}In-labeled DTPA-Bt(n)-BV (^{111}In-Bt$_{2.0}$-BV, ^{111}In-Bt$_{3.5}$-BV, or ^{111}In-Bt$_{7.1}$-BV) in normal ddY mice at 24 h after injection of 100 μL each aliquot (20 kBq/20 μg of mAb). To evaluate whether avidin could accelerate the blood clearance of ^{111}In-Bt(n)-BV, we injected 100 μL of avidin solution (9.0 μg/mouse, molar equivalent [eq] to that of BV; Wako Pure Chemical Industries, Osaka, Japan) at 24 h after ^{111}In-Bt(n)-BV administration. Radioactivity uptakes were determined at 3 h after avidin injection, that is, 27 h after ^{111}In-Bt(n)-BV injection.

Study 3: Effect of Avidin Dose on Biodistribution Profiles of ^{111}In-Bt$_{3.5}$-BV. Normal mice were injected with 100 μL solution of ^{111}In-Bt$_{3.5}$-BV (20 kBq/20 μg of mAb), and 24 h later, the mice were injected with serial amounts of avidin (0, 1/5, 1/2, 1, 2, 5 eq of BV). Radioactivity uptakes were evaluated at 3 h after the injection of avidin, that is, at 27 h after the ^{111}In-Bt$_{3.5}$-BV injection.

Study 4: Comparison of Biodistribution Profiles of ^{111}In−BV and ^{111}In-Bt$_{3.5}$-BV in Tumor Xenograft Mice. One-hundred microliters of ^{111}In−BV or ^{111}In-Bt$_{3.5}$-BV (20 kBq/20 μg of mAb) was injected into the tumor-bearing mice, and radioactivity uptakes were determined at 27 and 72 h postinjection. For the ^{111}In-Bt$_{3.5}$-BV group, 100 μL of avidin solution (9.0 μg/mouse, 1 eq of BV) was injected at 24 h after the ^{111}In-Bt3.5-BV administration.

Dose Escalation Studies of ^{90}Y-Bt$_{3.5}$-BV and ^{90}Y−BV. To determine the influence of avidin on the maximum tolerated dose (MTD) of ^{90}Y-labeled DTPA-Bt$_{3.5}$-BV (^{90}Y-Bt$_{3.5}$-BV), we performed escalating radioactivity dose studies of ^{90}Y-Bt$_{3.5}$-BV with avidin injection in normal mice (7.4−18.5 MBq/100−250 μL/mouse) and tumor-bearing mice (3.7−9.25 MBq/100−250 μL/mouse) in a comparison with ^{90}Y-labeled DTPA-BV (^{90}Y−BV). Avidin was intravenously injected at 24 h after the ^{90}Y-Bt$_{3.5}$-BV administration. The body weight of each mouse was monitored twice a week. The MTD was determined based on the death of mice or body weight loss exceeding 20%.

Therapeutic Study. When the tumors were fully established (200 ± 71 mm^3), we divided the mice into three groups (*n* = 8 per group). Group 1: Treated with ^{90}Y-Bt$_{3.5}$-BV (7.4 MBq/100 μL/mouse) followed by 1 eq. of avidin injection at 24 h postinjection. Group 2: Treated with ^{90}Y−BV (3.7 MBq/100 μL/mouse). Group 3: Untreated (control group). There was no significant difference in the initial tumor volume among the groups. The tumor volumes were determined twice
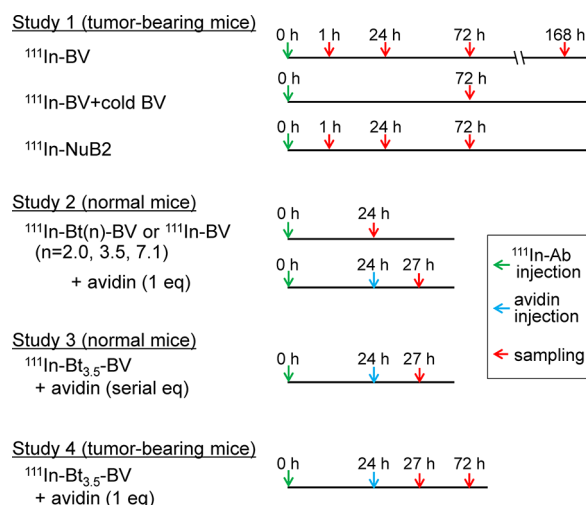

Figure 1. Summary of the biodistribution studies performed with ^{111}In-labeled mAbs. Study 1: Evaluation of biodistribution profiles and tumor specificity of ^{111}In−BV in MDA-MB-231 tumor xenograft mice. Study 2: Effect of biotin valency and clearing agent injection on the biodistribution profiles of ^{111}In-Bt(n)-BV in normal mice. Study 3: Effect of avidin dose on the biodistribution profiles of ^{111}In-Bt$_{3.5}$-BV in normal mice. Study 4: Comparison of the biodistribution profiles of ^{111}In−BV and ^{111}In-Bt$_{3.5}$-BV in tumor xenograft mice.
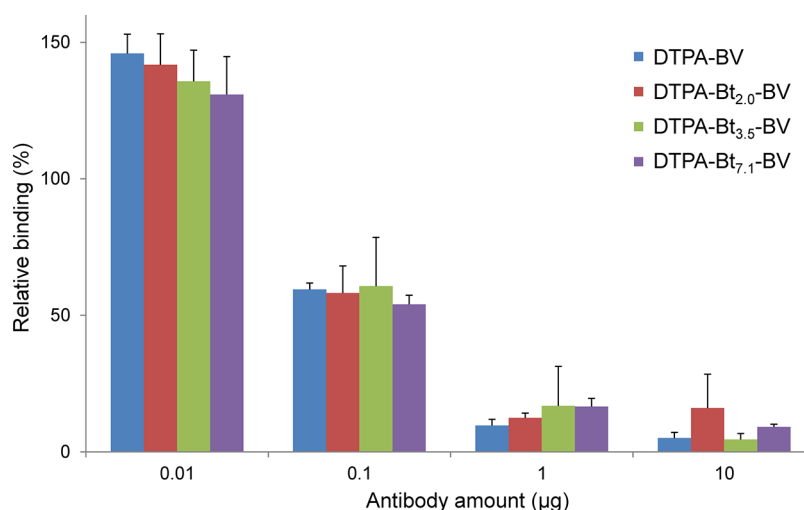
Figure 2. Immunoreactivity evaluation using $VEGF_{165}$-coated 96-well plates. Each value is the mean $\pm$ SD ($n = 4$).
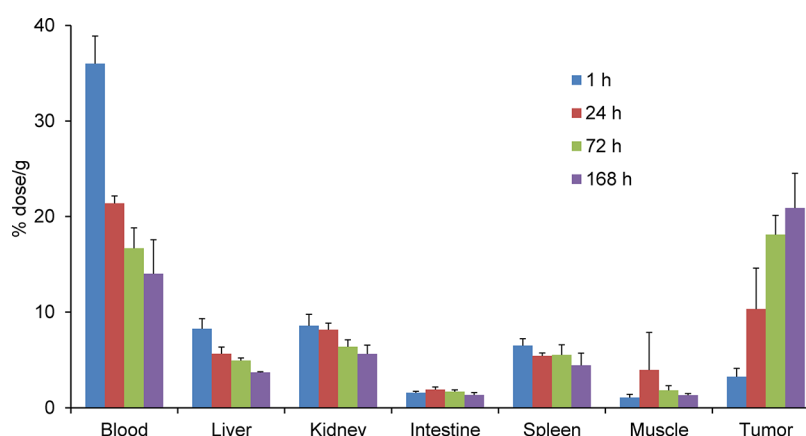

Figure 3. Biodistribution of radioactivity after the injection of ^{111}In$-$BV (protein dose: 20 μg) in the tumor-bearing mice. The biodistribution study data are mean $\pm$ SD ($n > 4$).

a week as described above. The observation was terminated when the tumor volume exceeded 2000 mm^3 or the mice were dead.

Statistical Analysis. Data are expressed as mean $\pm$ standard deviation (SD). For the comparison of the data of pairs of groups, Student's t-test was used. P-values < 0.05 were considered significant. GraphPad Prism software ver. 7 (GraphPad Software, La Jolla, CA) was used.

■ RESULTS

Analysis of Bt-BVs. The DTPA conjugation and biotin valencies (biotin number per mAb) of DTPA-Bt-BV (2.0−7.1) did not affect the binding affinity of BV to $VEGF_{165}$, as the immunoreactivity assay confirmed their maintained specificity (Figure 2).

Biodistribution Study. The biodistribution Study 1 demonstrated a high and specific tumor accumulation of the radiolabeled BV in the TNBC xenograft tumors. In the tumor-bearing mice, high tumor accumulation and retention of ^{111}In$-$BV were noted (Figure 3). The tumor uptake was significantly suppressed in the presence of the excess amount of unlabeled antibody (Figure S1, p < 0.05). The immunohistochemical analysis revealed the high expression level of VEGF in the MDA-MB-231 tumors (Figure S2). By contrast, ^{111}In-labeled anti-CD20 antibody showed significantly lower tumor accu-

mulation compared to ^{111}In$-$BV at 24 and 72 h after injection (Figure S3, p < 0.05). The biodistribution Study 1 also showed the high blood radioactivity levels of ^{111}In$-$BV even at 72 and 168 h after injection (Figure 3A, 16.7 $\pm$ 2.1 and 14.0 $\pm$ 3.6% ID/g, respectively) due to its slow blood clearance.

To determine whether the clearing agent injection could improve the slow blood clearance rate of BV, we next explored the influence of biotin valencies on the biodistribution patterns of ^{111}In-Bt(n)-BV in normal mice (Study 2). At 24 h after injection, the blood radioactivity levels of ^{111}In-Bt$_{2.0}$-BV and ^{111}In-Bt$_{3.5}$-BV were comparable to that of ^{111}In$-$BV, whereas that of ^{111}In-Bt$_{7.1}$-BV was significantly low (Figure 4A, p < 0.01). When avidin was injected subsequently to the tracers, the blood radioactivity level of ^{111}In-Bt$_{3.5}$-BV became significantly lower than that of ^{111}In$-$BV (Figure 4B, p < 0.01), whereas that of ^{111}In-Bt$_{2.0}$-BV remain unaffected.

We then explored the influence of the amount of avidin on the blood clearance enhancement of ^{111}In-Bt$_{3.5}$-BV (Study 3). Avidin decreased the blood radioactivity levels of ^{111}In-Bt$_{3.5}$-BV in a dose-dependent manner, but there was no significant difference between the levels of the 1 eq, 2 eq, and 5 eq groups (Figure 4C). On the basis of these results, we used the combination of ^{111}In-Bt$_{3.5}$-BV with 1 eq of avidin injection in the following biodistribution and therapeutic studies.
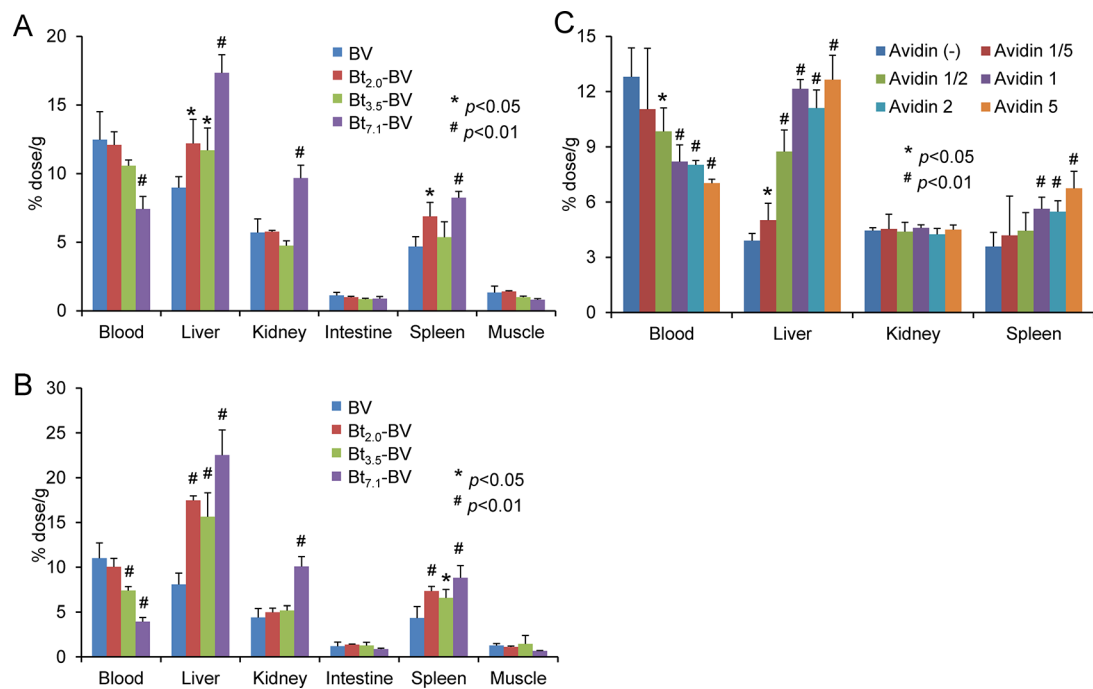
Figure 4. Biodistribution of the radioactivity of ^{111}In−BV or ^{111}In-Bt(n)-BV with avidin in normal mice. (A) 24 h after the injection of ^{111}In−BV or ^{111}In-Bt(n)-BV (mean ± SD, $n > 3$). Significant differences were observed between ^{111}In-Bt(n)-BV and ^{111}In−BV ($*p < 0.05$, $\#p < 0.01$). (B) 27 h after the injection of ^{111}In−BV or ^{111}In-Bt(n)-BV with 1 eq of avidin (mean ± SD, $n > 3$). Significant differences were observed between ^{111}In-Bt(n)-BV and ^{111}In−BV ($*p < 0.05$, $\#p < 0.01$). (C) 27 h after injection of ^{111}In-Bt$_{3.5}$-BV with increasing amount of avidin (mean ± SD, $n > 3$). Avidin injection significantly decreased the blood radioactivity levels and increased the liver and spleen radioactivity levels ($*p < 0.05$, $\#p < 0.01$).
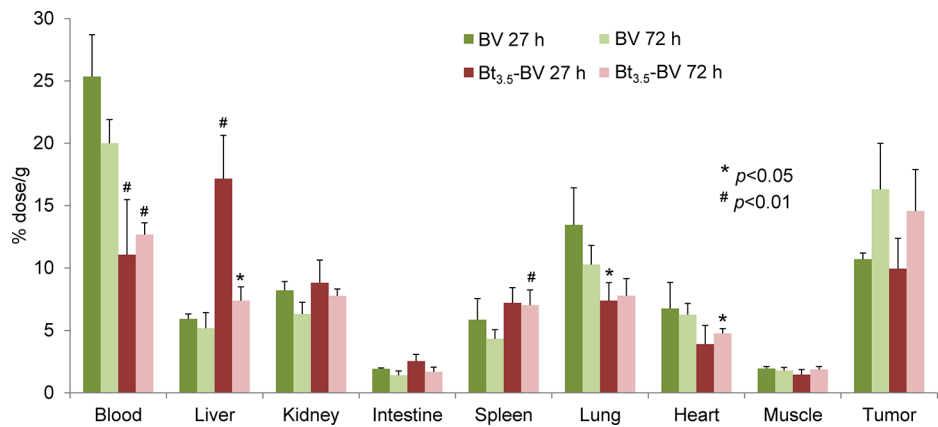

Figure 5. Biodistribution of radioactivity 27 and 72 h after the injection of ^{111}In−BV or ^{111}In-Bt$_{3.5}$-BV with 1 eq of avidin (mean ± SD, $n > 3$). The blood radioactivity levels of the ^{111}In-Bt$_{3.5}$-BV group were significantly lower than those of the ^{111}In−BV group ($*p < 0.05$, $\#p < 0.01$). There was no significant difference in tumor accumulation levels between the ^{111}In-Bt$_{3.5}$-BV group and ^{111}In−BV group.

Table 1. Escalating Radioactivity Dose Studies of ^{90}Y-Bt$_{3.5}$-BV with Avidin Injection and ^{90}Y−BV in Normal Mice and Tumor-Bearing Mice[a]

dose/mouse (MBq)		3.7	5.55	7.4	9.25	11.1	12.95	14.8	16.65	18.5
normal mice	^{90}Y−BV	−[c]	−	4/4	4/4[b]	3/4	1/4	−	−	−
	^{90}Y-Bt$_{3.5}$-BV	−	−	−	4/4	4/4[b]	2/4	1/4	0/4	0/2
tumor-bearing mice	^{90}Y−BV	5/5[b]	3/5	1/4	−	−	−	−	−	−
	^{90}Y-Bt$_{3.5}$-BV	3/3	3/3	3/3[b]	0/3	−	−	−	−	−

[a]Each value represents the number of survived mice/total mice at each dose. [b]MTD was determined as the highest dose at which no mice died. [c]−: not tested.

This combination also accelerated the blood clearance of ^{111}In-Bt$_{3.5}$-BV in the MDA-MB-231 xenograft mice (Figure 5).

At 27 h after injection, the radioactivity level in the blood of the ^{111}In-Bt$_{3.5}$-BV group was significantly lower than that of the
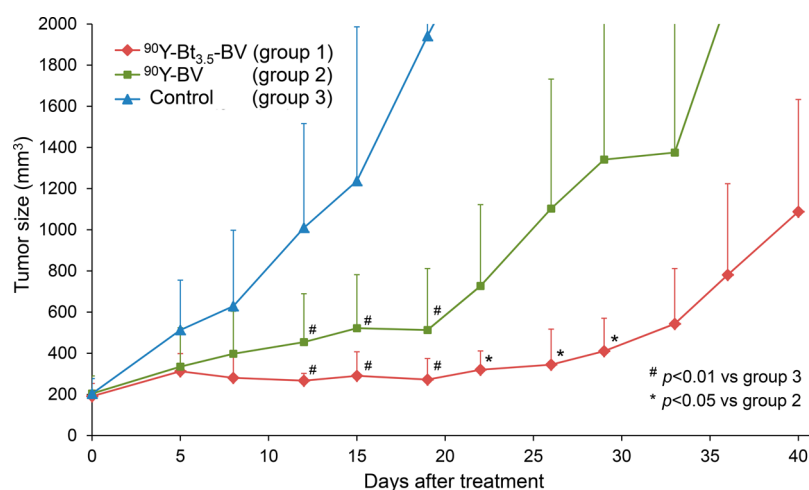
Figure 6. Therapeutic effect of ^{90}Y−BV or ^{90}Y-Bt$_{3.5}$-BV in tumor-bearing mice (mean ± SD, $n > 6$). Tumor growth was significantly inhibited in both the ^{90}Y−BV- and ^{90}Y-Bt$_{3.5}$-BV-treated mice compared to the untreated control mice (#$p < 0.01$). The tumor volume of the ^{90}Y-Bt$_{3.5}$-BV group was significantly smaller than that of the ^{90}Y−BV group from day 22 to day 29 (∗$p < 0.05$).

^{111}In−BV group (11.1 ± 4.4%dose/g vs 25.4 ± 3.4%dose/g, respectively, $p < 0.01$). No significant difference was observed in tumor radioactivity levels between the ^{111}In-Bt$_{3.5}$-BV group and ^{111}In−BV group (9.9 ± 2.4%dose/g and 10.7 ± 0.5%dose/g, respectively). The tumor to blood ratio of ^{111}In-Bt$_{3.5}$-BV group became higher than that of ^{111}In−BV group (1.10 ± 0.73 vs 0.43 ± 0.04, respectively) though the difference was not statistically significant. The avidin injection significantly raised the radioactivity levels in the liver (17.2 ± 3.5%dose/g and 5.9 ± 0.4%dose/g, respectively, $p < 0.01$).

The effective dose of ^{90}Y−BV and ^{90}Y-Bt$_{3.5}$-BV estimated from biodistribution data was 0.797 and 0.753 mSv/MBq, respectively. The estimated absorbed dose of ^{90}Y−BV and ^{90}Y-Bt$_{3.5}$-BV to the red marrow was 0.197 and 0.125 mSv/MBq, respectively, and that to the liver was 1.27 and 1.74 mSv/MBq, respectively.

Therapeutic Study. The escalating radioactivity dose studies revealed that the avidin injection could widen the applicable range of ^{90}Y-Bt$_{3.5}$-BV. In both the normal mice and the tumor-bearing mice, the MTD of ^{90}Y-Bt$_{3.5}$-BV with the avidin injection was higher than that of ^{90}Y−BV (11.1 MBq vs 9.25 MBq in the normal mice, and 7.4 MBq vs 3.7 MBq in the tumor-bearing mice, respectively, Table 1). Therefore, in the subsequent therapeutic study, we administered 7.4 MBq of ^{90}Y-Bt$_{3.5}$-BV or 3.7 MBq of ^{90}Y−BV to the mice in each group. Tumor growth was significantly suppressed in both treatment groups compared to that of the control group (Figure 6, $p < 0.01$). In particular, the tumor volume of group 1 (^{90}Y-Bt$_{3.5}$-BV with avidin) was significantly smaller than that of group 2 (^{90}Y−BV) at 22, 26, and 29 days after treatment ($p < 0.05$, Figure 6). Two of the eight mice in group 1 and one of the eight mice in group 2 died approximately 3 weeks after treatment.

■ DISCUSSION

The high and persistent accumulation of ^{111}In−BV observed in the VEGF-positive TNBC tumor (MDA-MB-231) xenograft supports RIT with BV as an attractive candidate for TNBC treatment, though the indication of unlabeled BV for breast cancer was withdrawn by the U.S. Food and Drug Administration (FDA) in 2011 based on the lack of overall survival improvement.[26,36] At the same time, the slow blood clearance of ^{111}In−BV, which is consistent with previous

studies,[5,13] confirmed the necessity of a blood clearance enhancement strategy.

The present normal mice studies demonstrated that the avidin chase worked efficiently to enhance the blood clearance of ^{111}In−BV, and an appropriate biotin valency is a responsible factor for the success of the avidin chase. All Bt-BVs maintained the binding affinity to VEGF$_{165}$, whereas seven-biotin functionalization (^{111}In-Bt$_{7.1}$-BV) greatly altered the biodistribution pattern of ^{111}In−BV. Khawli et al. suspected that the reduced net charge of antibody by biotinylation of ε-amino groups of lysine residues is the factor responsible for the enhanced blood clearance.[37] As the number of biotins increases, ^{111}In-Bt-BVs would have become more susceptible to being recognized as a foreign substance since the accumulation level of ^{111}In-Bt-BVs in the liver, kidney, and spleen became higher with the increase in the number of biotins. The use of Bt$_{7.1}$-BV as an RIT agent thus would be inappropriate since increased off-target distribution inevitably decreases the tumor accumulation level. Too small a biotin valency is, by contrast, also inappropriate. Although the avidin injection in the present study decreased the blood radioactivity level of ^{111}In-Bt$_{3.5}$-BV, it did not affect the blood radioactivity level of ^{111}In-Bt$_{2.0}$-BV. This is presumably because a certain number of biotin functionalization was necessary to effectively eliminate BV from the systemic circulation by enabling the avidin(s) to readily conjugate with each BV molecule.

The optimized dose of avidin injection successfully accelerated the blood clearance of ^{111}In-Bt$_{3.5}$-BV without impairing its tumor accumulation level. The equivalent amount of avidin to Bt$_{3.5}$-BV turned out to be sufficient to suppress the blood radioactivity level in the normal mice study. This is excessive (by four-times) compared to the amount of Bt$_{3.5}$-BV that remained in the circulation at 24 h after injection, considering the blood radioactivity levels of ^{111}In-Bt$_{3.5}$-BV (approximately 25% dose, assuming that the blood volume of mice is 2 mL). This result was inconsistent with previous observation that reported more than 10-times excess amount of avidin injection does-dependently accelerate the blood clearance of radiolabeled biotinylated antibodies.[20,38] The discrepancy may be due to the difference in the nature of antibodies, biotin valencies, or radiolabeling method used in these studies. We finally selected 1 eq of avidin since the

necessary sufficient amount should be used to avoid the possibility that surplus avidin may bind and remove the antibodies already accumulated in the tumor. Further reduction in the blood radioactivity level was not observed at 3 h after the avidin injection (up to 24 h, data not shown) as previously reported, probably because avidin itself was rapidly eliminated from the circulation.[19,25]

The accelerated blood clearance by avidin chase successfully minimized the radiation exposure to bone marrow, the dose-limiting organ. The lowered estimated absorbed dose to the red marrow in the avidin chase group (0.197 vs 0.125 mSv/MBq) indicates the increased therapeutic index in those mice 1.5-times more than mice without avidin chase. The accelerated blood clearance instead increased the radioactivity level accumulated in the liver. The clearance rate from the liver was much slower than what has been reported for radioiodine labeled antibodies due to the residualizing nature of radio-metal.[39] One concern regarding increased radioactivity accumulation is the liver toxicity. However, the estimated absorbed dose to the liver was increased by only 1.37-times between mice with or without avidin chase and thus would be acceptable. When 3.75-times higher dose ^{90}Y-ibritumomab tiuxetan RIT with autologous stem cell transplantation was applied, no liver toxicity developed in the patient who received a dose of 25 Gy to the liver, the dose limiting organ in their study.[40]

As expected, the avidin injection enabled the increase in the MTD of ^{90}Y-Bt$_{3.5}$-BV to twice as much as that of ^{90}Y−BV in tumor-bearing mice, which consequently improved the therapeutic effect of ^{90}Y-Bt$_{3.5}$-BV by increasing the absorbed dose to the tumor. To our knowledge, this is the first study that demonstrated the usefulness of avidin chase for increasing the MTD and dramatically potentiating the therapeutic effect of ^{90}Y−BV. The avidin chase strategy has yet to be applied in clinic, but it is worth investigating the potential effect for tumor treatment in future clinical studies. Further studies using various solid tumor models are desirable to confirm the applicability of this strategy. Even though the tumors were not completely eradicated, the avidin chase strategy is simple compared with extracorporeal depletion and effective to raise the absorbed dose to the tumor without increasing side effects, and it is thereby compatible with any other treatment strategies such as chemotherapy, radiosensitizers, or fractionated RIT. To further improve the therapeutic outcomes, investigations of the optimum combination of treatment strategies would be the objective of the future research.

In spite of the therapeutic benefit of pretargeting RIT with avidin−biotin system, it has received little attention due to the immunogenicity of streptavidin.[41] Contrary to the pretargeting RIT, severe allergic reaction would not be expected in the avidin chase strategy because avidin is injected only one time, yet immunogenicity of avidin is still a subject of concern for clinical use. Some chemical or genetical modification of avidin, or the use of other type of avidin derived from different species, may eventually eliminate the concern related to the immunogenicity.[42,43]

There were some limitations in this study. First, we used only one cell line. Although the use of other cell lines would affect the therapeutic effect, it would be irrelevant to the blood clearance acceleration effect and the tumor absorbed dose enhancement effect of the avidin chase. Therefore, this strategy has great potential to improve the therapeutic effect of BV-RIT for any type of VEGF-expressing tumors. Second, further

optimization such as the dose and timing of the avidin injection is necessary to apply this method in clinical practice. However, considering its simplicity compared with the conventional pretargeting strategies, clinical applications of the avidin chase would be more feasible.

■ CONCLUSION

The avidin chase successfully accelerated the blood clearance of ^{111}In-labeled biotinylated-bevacizumab without impairing its tumor accumulation level. This strategy also increased the MTD of ^{90}Y-bevacizumab, and consequently improved the therapeutic effect. These results underscored the potential usefulness of ^{90}Y-bevacizumab RIT with the avidin chase for the treatment of VEGF-positive tumors.

■ ASSOCIATED CONTENT

ⓈSupporting Information

The Supporting Information is available free of charge on the ACS Publications website at DOI: 10.1021/acs.molpharmaceut.8b00027.

Biodistribution of ^{111}In−BV with unlabeled antibody, immunohistochemical analysis, and biodistribution of ^{111}In-NuB2 (PDF)

■ AUTHOR INFORMATION

Corresponding Author

*E-mail: hanaokah@gunma-u.ac.jp. Phone: +81-27-220-8403. Fax: +81-27-220-8409.

ORCID ⓘ

Hirofumi Hanaoka: 0000-0003-2421-7397

Notes

The authors declare no competing financial interest.

■ ACKNOWLEDGMENTS

■ REFERENCES

(1) Song, H.; Sgouros, G. Radioimmunotherapy of solid tumors: searching for the right target. *Curr. Drug Delivery* **2011**, *8* (1), 26−44.

(2) Larson, S. M.; Carrasquillo, J. A.; Cheung, N. K.; Press, O. W. Radioimmunotherapy of human tumours. *Nat. Rev. Cancer* **2015**, *15* (6), 347−60.

(3) Neufeld, G.; Cohen, T.; Gengrinovitch, S.; Poltorak, Z. Vascular endothelial growth factor (VEGF) and its receptors. *FASEB J.* **1999**, *13* (1), 9−22.

(4) Hanahan, D.; Weinberg, R. A. Hallmarks of cancer: the next generation. *Cell* **2011**, *144* (5), 646−74.

(5) Nagengast, W. B.; de Vries, E. G.; Hospers, G. A.; Mulder, N. H.; de Jong, J. R.; Hollema, H.; Brouwers, A. H.; van Dongen, G. A.; Perk, L. R.; Lub-de Hooge, M. N. In vivo VEGF imaging with radiolabeled bevacizumab in a human ovarian tumor xenograft. *J. Nucl. Med.* **2007**, *48* (8), 1313−9.

(6) Paudyal, B.; Paudyal, P.; Oriuchi, N.; Hanaoka, H.; Tominaga, H.; Endo, K. Positron emission tomography imaging and biodistribution of vascular endothelial growth factor with ^{64}Cu-labeled bevacizumab in colorectal cancer xenografts. *Cancer Sci.* **2011**, *102* (1), 117−21.

(7) Gaykema, S. B. M.; Brouwers, A. H.; Lub-de Hooge, M. N.; Pleijhuis, R. G.; Timmer-Bosscha, H.; Pot, L.; van Dam, G. M.; van der Meulen, S. B.; de Jong, J. R.; Bart, J.; de Vries, J.; Jansen, L.; de Vries, E. G.; Schröder, C. P. ^{89}Zr-bevacizumab PET imaging in primary breast cancer. *J. Nucl. Med.* **2013**, *54* (7), 1014−8.

(8) Rizvi, S. M. A.; Song, E. Y.; Raja, C.; Beretov, J.; Morgenstern, A.; Apostolidis, C.; Russell, P. J.; Kearsley, J. H.; Abbas, K.; Allen, B. J. Preparation and testing of bevacizumab radioimmunoconjugates with bismuth-213 and bismuth-205/bismuth-206. *Cancer Biol. Ther.* **2008**, *7* (10), 1547−54.

(9) Xiao, J.; Xu, X.; Li, X.; Li, Y.; Liu, G.; Tan, H.; Shen, H.; Shi, H.; Cheng, D. Re-188 enhances the inhibitory effect of bevacizumab in non-small-cell lung cancer. *Molecules* **2016**, *21* (10), 1308.

(10) Ferrara, N.; Hillan, K. J.; Novotny, W. Bevacizumab (Avastin), a humanized anti-VEGF monoclonal antibody for cancer therapy. *Biochem. Biophys. Res. Commun.* **2005**, *333* (2), 328−335.

(11) Roviello, G.; Bachelot, T.; Hudis, C. A.; Curigliano, G.; Reynolds, A. R.; Petrioli, R.; Generali, D. The role of bevacizumab in solid tumours: A literature based meta-analysis of randomised trials. *Eur. J. Cancer* **2017**, *75*, 245−58.

(12) Holliger, P.; Hudson, P. J. Engineered antibody fragments and the rise of single domains. *Nat. Biotechnol.* **2005**, *23* (9), 1126−36.

(13) Lin, Y. S.; Nguyen, C.; Mendoza, J. L.; Escandon, E.; Fei, D.; Meng, Y. G.; Modi, N. B.; et al. Preclinical pharmacokinetics, interspecies scaling, and tissue distribution of a humanized monoclonal antibody against vascular endothelial growth factor. *J. Pharmacol. Exp. Ther.* **1999**, *288* (1), 371−8.

(14) Gordon, M. S.; Margolin, K.; Talpaz, M.; Sledge, G. W., Jr.; Holmgren, E.; Benjamin, R.; Stalter, S.; Shak, S.; Adelman, D. Phase I safety and pharmacokinetic study of recombinant human anti-vascular endothelial growth factor in patients with advanced cancer. *J. Clin. Oncol.* **2001**, *19* (3), 843−50.

(15) Li, D.; Liu, S.; Liu, R.; Zhou, Y.; Park, R.; Naga, K.; Krasnoperov, V.; Gill, P. S.; Li, Z.; Shan, H.; Conti, P. S. EphB4-targeted imaging with antibody h131, h131-F(ab′)2 and h131-Fab. *Mol. Pharmaceutics* **2013**, *10* (12), 4527−33.

(16) Xenaki, K. T.; Oliveira, S.; van Bergen En Henegouwen, P. M. P. Antibody or antibody fragments: Implications for molecular imaging and targeted therapy of solid tumors. *Front. Immunol.* **2017**, *8*, 1287.

(17) Goldenberg, D. M.; Sharkey, R. M.; Paganelli, G.; Barbet, J.; Chatal, J. F. Antibody pretargeting advances cancer radioimmunodetection and radioimmunotherapy. *J. Clin. Oncol.* **2006**, *24* (5), 823−34.

(18) Green, D. J.; Press, O. W. Whither Radioimmunotherapy: To be or not to be? *Cancer Res.* **2017**, *77* (9), 2191−6.

(19) Liu, G.; Dou, S.; Chen, X.; Chen, L.; Liu, X.; Rusckowski, M.; Hnatowich, D. J. Adding a clearing agent to pretargeting does not lower the tumor accumulation of the effector as predicted. *Cancer Biother.Radiopharm.* **2010**, *25* (6), 757−62.

(20) Kobayashi, H.; Sakahara, H.; Hosono, M.; Yao, Z. S.; Toyama, S.; Endo, K.; Konishi, J. Improved clearance of radiolabeled biotinylated monoclonal antibody following the infusion of avidin as a ″chase″ without decreased accumulation in the target tumor. *J. Nucl. Med.* **1994**, *35* (10), 1677−84.

(21) Mårtensson, L.; Nilsson, R.; Ohlsson, T.; Sjögren, H. O.; Strand, S. E.; Tennvall, J. Reduced myelotoxicity with sustained tumor concentration of radioimmunoconjugates in rats after extracorporeal depletion. *J. Nucl. Med.* **2007**, *48* (2), 269−76.

(22) Begent, R. H.; Keep, P. A.; Green, A. J.; Searle, F.; Bagshawe, K. D.; Jewkes, R. F.; Jones, B. E.; Barratt, G. M.; Ryman, B. E. Liposomally entrapped second antibody improves tumour imaging with radiolabelled (first) antitumour antibody. *Lancet* **1982**, *320* (8301), 739−42.

(23) Sato, N.; Saga, T.; Sakahara, H.; Nakamoto, Y.; Zhao, S.; Kuroki, M.; Iida, Y.; Endo, K.; Konishi, J. Avidin chase can reduce myelotoxicity associated with radioimmunotherapy of experimental liver micrometastases in mice. *Jpn. J. Cancer Res.* **2000**, *91* (6), 622−8.

(24) Li, G. P.; Wang, Y. X.; Huang, K.; Zhang, H.; Zhang, C. F. Avidin chase reduces side effects of radioimmunotherapy in nude mice bearing human colon carcinoma. *World J. Gastroenterol.* **2005**, *11* (13), 1917−21.

(25) Mirallié, E.; Saï-Maurel, C.; Faivre-Chauvet, A.; Regenet, N.; Chang, C. H.; Goldenberg, D. M.; Chatal, J. F.; Barbet, J.; Thedrez, P. Improved pretargeted delivery of radiolabelled hapten to human tumour xenograft in mice by avidin chase of circulating bispecific antibody. *Eur. J. Nucl. Med. Mol. Imaging* **2005**, *32* (8), 901−9.

(26) Tolaney, S. M.; Boucher, Y.; Duda, D. G.; Martin, J. D.; Seano, G.; Ancukiewicz, M.; Barry, W. T.; Goel, S.; Lahdenrata, J.; Isakoff, S. J.; Yeh, E. D.; Jain, S. R.; Golshan, M.; Brock, J.; Snuderl, M.; Winer, E. P.; Krop, I. E.; Jain, R. K. Role of vascular density and normalization in response to neoadjuvant bevacizumab and chemotherapy in breast cancer patients. *Proc. Natl. Acad. Sci. U. S. A.* **2015**, *112* (46), 14325−30.

(27) Jerusalem, G.; Lousberg, L.; Schroeder, H.; Collignon, J. Triple-negative breast cancer: treatment challenges and solutions. *Breast Cancer: Targets Ther.* **2016**, *8*, 93−107.

(28) Sakahara, H.; Endo, K.; Nakashima, T.; Koizumi, M.; Ohta, H.; Torizuka, K.; Furukawa, T.; Ohmomo, Y.; Yokoyama, A.; Okada, K.; Yoshida, O.; Nishi, S. Effect of DTPA conjugation on the antigen binding activity and biodistribution of monoclonal antibodies against alpha-Fetoprotein. *J. Nucl. Med.* **1985**, *26* (7), 750−5.

(29) Green, N. M. A spectrophotometric assay for avidin and biotin based on binding of dyes by avidin. *Biochem. J.* **1965**, *94*, 23c−24c.

(30) Hunter, W. N.; Greenwood, F. C. Preparation of iodine-131 labeled human growth hormone of high specific activity. *Nature* **1962**, *194*, 495−6.

(31) Chang, A. J.; Sohn, R.; Lu, Z. H.; Arbeit, J. M.; Lapi, S. E. Detection of rapalog-mediated therapeutic response in renal cancer xenografts using ^{64}Cu-bevacizumab immunoPET. *PLoS One* **2013**, *8* (3), e58949.

(32) Kurebayashi, J.; Otsuki, T.; Kunisue, H.; Mikami, Y.; Tanaka, K.; Yamamoto, S.; Sonoo, H. Expression of vascular endothelial growth factor (VEGF) family members in breast cancer. *Jpn. J. Cancer Res.* **1999**, *90* (9), 977−81.

(33) Hnatowich, D. J.; Virzi, F.; Doherty, P. W. DTPA-coupled antibodies labeled with yttrium-90. *J. Nucl. Med.* **1985**, *26* (5), 503−9.

(34) Roselli, M.; Schlom, J.; Gansow, O. A.; Raubitschek, A.; Mirzadeh, S.; Brechbiel, M. W.; Colcher, D. Comparative biodistributions of yttrium and indium-labeled monoclonal antibody B72.3 in athymic mice bearing human colon carcinoma xenografts. *J. Nucl. Med.* **1989**, *30* (5), 672−82.

(35) Stabin, M. G.; Sparks, R. B.; Crowe, E. OLINDA/EXM: the second generation personal computer software for internal dose assessment in nuclear medicine. *J. Nucl. Med.* **2005**, *46* (6), 1023−7.

(36) *Decision of the Commissioner. Proposal to Withdraw Approval for the Breast Cancer Indication for Avastin (Bevacizumab)*; U.S. Food and Drug Administration, 2011.

(37) Khawli, L. A.; Mizokami, M. M.; Sharifi, J.; Hu, P.; Epstein, A. L. Pharmacokinetic characteristics and biodistribution of radioiodinated chimeric TNT-1, −2, and −3 monoclonal antibodies after chemical modification with biotin. *Cancer Biother.Radiopharm.* **2002**, *17* (4), 359−70.

(38) Petronzelli, F.; Pelliccia, A.; Anastasi, A. M.; D'Alessio, V.; Albertoni, C.; Rosi, A.; Leoni, B.; De Angelis, C.; Paganelli, G.; Palombo, G.; Dani, M.; Carminati, P.; De Santis, R. Improved tumor targeting by combined use of two antitenascin antibodies. *Clin. Cancer Res.* **2005**, *11* (19 Pt 2), 7137s−7145s.

(39) Arano, Y.; Mukai, T.; Uezono, T.; Wakisaka, K.; Motonari, H.; Akizawa, H.; Taoka, Y.; Yokoyama, A. A biological method to evaluate bifunctional chelating agents to label antibodies with metallic radionuclides. *J. Nucl. Med.* **1994**, *35* (5), 890−8.

(40) Cremonesi, M.; Ferrari, M.; Grana, C. M.; Vanazzi, A.; Stabin, M.; Bartolomei, M.; Papi, S.; Prisco, G.; Ferrucci, P. F.; Martinelli, G.; Paganelli, G. High-dose radioimmunotherapy with ^{90}Y-ibritumomab tiuxetan: comparative dosimetric study for tailored treatment. *J. Nucl. Med.* **2007**, *48* (11), 1871−9.

(41) Altai, M.; Membreno, R.; Cook, B.; Tolmachev, V.; Zeglis, B. M. Pretargeted imaging and therapy. *J. Nucl. Med.* **2017**, *58* (10), 1553−9.

(42) Chinol, M.; Casalini, P.; Maggiolo, M.; Canevari, S.; Omodeo, E. S.; Caliceti, P.; Veronese, F. M.; Cremonesi, M.; Chiolerio, F.; Nardone, E.; Siccardi, A. G.; Paganelli, G. Biochemical modifications of avidin improve pharmacokinetics and biodistribution, and reduce immunogenicity. *Br. J. Cancer* **1998**, *78* (2), 189−97.

(43) Helppolainen, S. H.; Nurminen, K. P.; Määttä, J. A.; Halling, K. K.; Slotte, J. P.; Huhtala, T.; Liimatainen, T.; Ylä-Herttuala, S.; Airenne, K. J.; Närvänen, A.; Jänis, J.; Vainiotalo, P.; Valjakka, J.; Kulomaa, M. S.; Nordlund, H. R. Rhizavidin from Rhizobium etli: the first natural dimer in the avidin protein family. *Biochem. J.* **2007**, *405* (3), 397−405.
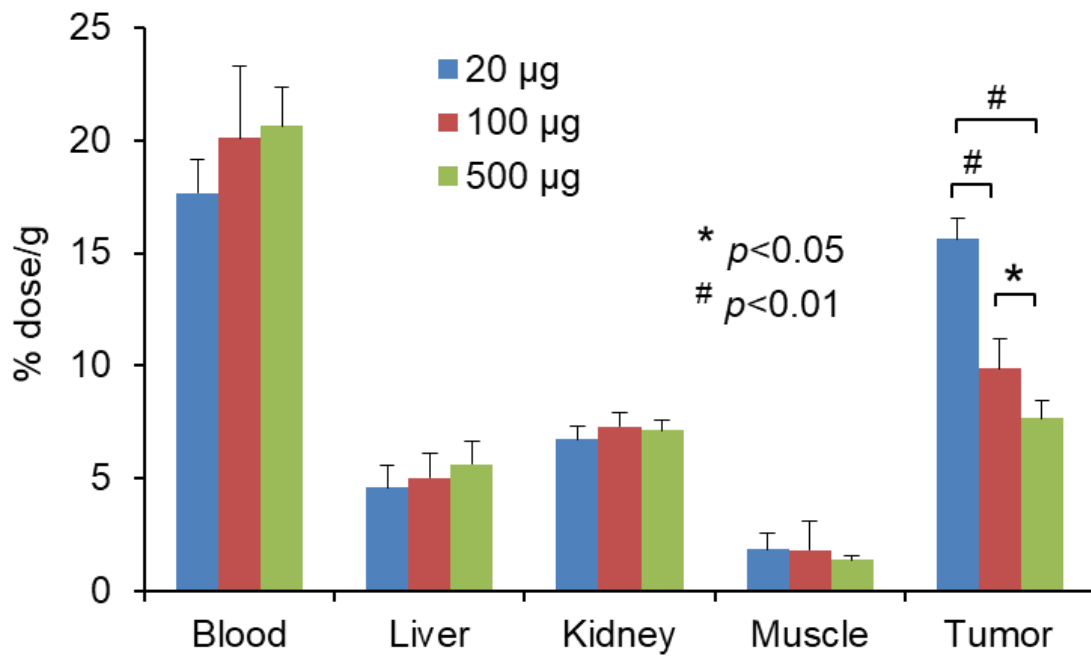
Figure S1. The biodistribution of radioactivity 72 h after the injection of ^{111}In-BV with different amounts of unlabeled antibody (20, 100, or 500 μg/mouse) in the tumor-bearing mice. The tumor accumulation level of ^{111}In-B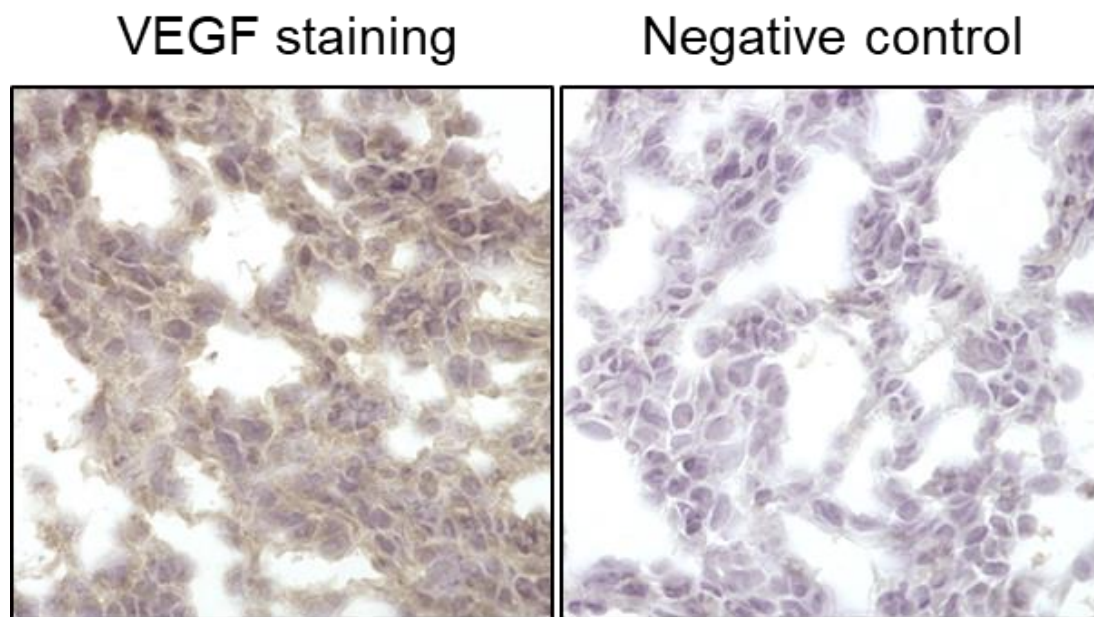V was significantly decreased in a dose-dependent manner (*p<0.05, #p<0.01). The biodistribution study data are mean ± SD (n>4).

Figure S2. Microscopy images (×40) of an MDA-MB-231 tumor frozen section stained
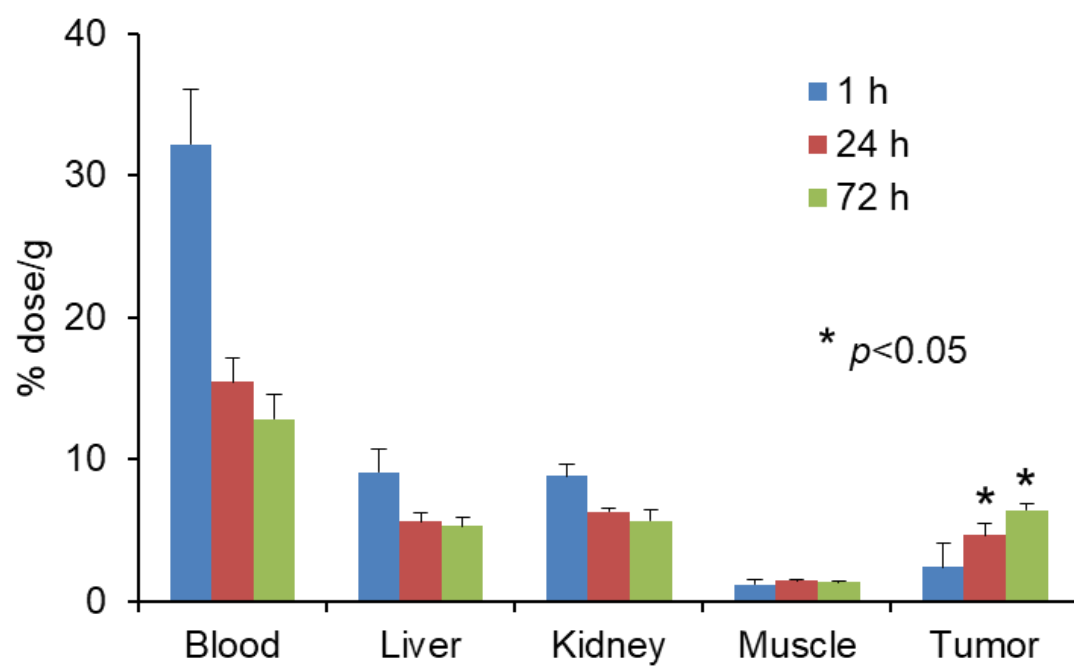
with anti-VEGF antibody.

Figure S3. The biodistribution of radioactivity after the injection of ^{111}In-NuB2 in the tumor-bearing mice. The tumor accumulation levels of ^{111}In-NuB2 were significantly lower than those of ^{111}In-BV (*$p<0.05$). The biodistribution study data are mean ± SD ($n>4$).